Electronic Supplementary Material (ESI) for ChemComm.

Electronic supplementary information

Double zipper helical assembly of deoxyoligonucleotides: mutual templating and chiral imprinting to form hybrid DNA ensembles

Nagarjun Narayanaswamy,[a] Gorle Suresh,[b] U. Deva Priyakumar,[b] and T. Govindaraju*[a]

[a]Bioorganic Chemistry Laboratory, New Chemistry Unit, Jawaharlal Nehru Centre for Advanced Scientific Research, Jakkur P.O., Bangalore 560064, Karnataka, India. Email: tgraju@jncasr.ac.in

[b]Centre for Computational Natural Sciences and Bioinformatics, International Institute of Information Technology, Hyderabad 500032, India.

Materials and Methods

***General*:** Perylene-3,4,9,10-tetracarboxylicdianhydride (PDA), deoxyoligonucleotides (dB_n/oligos: dA_{10}, dT_{10}, dA_{20}, dT_{20}, dG_{10}, dG_{20}, dC_{10}, dC_{20}), phosphate buffered saline (PBS) and 2-bromo-ethylamine hydrogen bromide were purchased from Sigma–Aldrich. Di-*tert*-butyl dicarbonate and adenine were obtained from Spectrochem Pvt. Ltd. Mumbai (India). All other reagents were used as received unless otherwise mentioned. ^{1}H and ^{13}C-NMR spectra were recorded on a Bruker AV-400 spectrometer with chemical shifts reported as ppm (in $CDCl_3$/DMSO-d_6, tetramethylsilane as internal standard) at 20 ºC. UV-vis and CD spectra of samples were analyzed in quartz cuvette of 1 mm path length. High resolution mass spectra (HRMS) were obtained on Agilent Technologies 6538 UHD Accurate-Mass Q-TOF LC/MS spectrometer.

Sample preparation for UV-vis and CD measurements. Samples for UV-vis and CD measurements were prepared by dissolving **APA** in DMSO with trace amount of trifluoroacetic acid in the order of 10^{-3} M. Oligo-stock solutions were prepared by dissolving the oligos in double deionized water in the order of 10^{-4} M. Double zipper assembly (hybrid DNA ensembles) of oligos were effected by adding the **APA** (in DMSO) in PBS-buffer solution (10 mM, pH = 7, 10% DMSO) and subjected to annealing by heating the sample to 85 °C for 15 min followed by cooling the sample solutions to room temperature for 7 h, stored in refrigerator for 4 h.

UV-vis absorption spectroscopy. The UV–vis absorption spectra were recorded on a Perkin Elmer Model Lambda 900 spectrophotometer at ambient conditions i.e., 25 °C. Temperature dependent measurements were carried out on Cary 500 UV-vis-NIR spectrophotometer equipped with Cary temperature controller in the range of 20 °C to 90 °C with ramp rate of 1 ^{o}C/min. A

blank sample containing PBS buffer solution (10 mM, pH = 7, 10% DMSO) was recorded and subtracted from the collected data.

Circular Dichroism (CD) spectroscopy. CD experiments were carried out on a Jasco J-815 spectrometer under nitrogen atmosphere to avoid water condensation. Temperature dependent measurements were performed employing Peltier-type temperature controller (CDF-4265/15) in the range of 20 °C to 90 °C with a ramp rate of 1 ^{o}C/min. Scans were performed over the wavelength range of 250-700 nm with a speed of 200 nm/min and the spectra represent an average of three scans. A blank sample containing PBS buffer solution was recorded and subtracted from the collected data.

Thermal denaturation studies**:** Thermal denaturation curves of oligos in presence of **APA** (hybrid DNA ensembles) were recorded in the 10–90 °C range with heating rate 1 °C/min. The variable temperature/wavelength mode was used. CD signal was recorded at 560 nm and the complete CD spectra were recorded in the wavelength region of 250–700 nm with data collection for every 5 °C. Melting temperatures (T_m) of hybrid DNA ensembles [dB_n-(**APA**)$_n$-dB_n] were calculated from the first derivative curve of the molar ellipticity change vs. temperature.

Atomic force microscopy (AFM): AFM measurements were performed on Bruker AFM instrument under ambient conditions. Preformed complexes of **APA** and dT_{20} were prepared by drop casting the sample solutions on the silicon (111) surface and air dried. AFM section analysis was done offline.

Additional information for NMR-spectra: **APA** exhibit strong π-π and hydrogen bonding interaction attributed to central perylene core and adenine moieties. Unlike our mutual

templating studies of **APA** and dB_n where we use relatively lower concentrations of **APA**, we need much higher concentration of **APA** for NMR study. At higher concentration (milligrams quantity) solubility of **APA** was poor. To enhance its solubility and to obtain good spectra we added trace amount of trifluoroacetic acid (TFA). It is known that TFA acts as hydrogen bond breaker (e.g., in case of many peptides). Thus, we were able to record good ^{1}H and ^{13}C NMR spectra. NMR peaks at 110.7, 113.6, 116.4, 119.3, 157.8, 158.3, 158.6 and 159.0 *ppm* corresponding TFA in ^{13}C and are not reported in the ^{13}C-NMR data of **APA**.

***Stoichiometry of APA:dB$_n$* complexation to form DNA ensembles**: In general, analysis of reported DNA-templated self-assembly reveal 100% binding efficiency of guest (**APA**) to host (DNA) can be achieved only if the relative number of guest (φ_g) are greater than the host binding sites (φ_h), i.e $\eta = \varphi_g / \varphi_h > 1$.[1] Therefore, to validate our proposed stoichiometric ratio of **APA**:dB_{10} (10:2), we performed the concentration dependent CD studies of fixed concentration of dB_n with increasing concentration of **APA**. In this experiment, we recorded CD spectra of performed complexes of **APA**:dT_{10} with increasing concentration of **APA** from 0 to 70 µM. Upon increasing concentration of **APA** from 0 to 50 µM, CD spectra showed an increase in CD signal intensity in the perylene absorption region (400-600 nm) with fixed concentration of dT_{10} (10 µM) (i.e A:T = 0:1 to 1:1). With further increase in concentration of **APA** from 50 to 70 µM, CD signal in perylene absorption region reaches saturation for A:T ≥ 1:1. These results showed the saturation of CD signal at greater than 50 µM which indicates $\eta = \varphi_g / \varphi_h > 1$.

Computational studies: All the model systems were built using Gauss View 05 [2] and Visual Molecular Dynamics (VMD) [3] softwares. Initially perylenebisimide (PBI) monomer was built, and optimized at the M06 level [4] along with the 6-31+G* basis set using the Gaussian 09 suite of

programs [5] and using semi empirical PM7 level of theory [6] using the MOPAC2012 program.[7] M06 and PM7 methods were chosen since they have been shown to account for dispersion type non-bonded interactions.[8] PBI and **APA** monomers, and respective dimers were built using the optimized PBI molecule in Gauss View 05. PBI dimer was modeled by placing the optimized structures of the two identical monomers such that the interplanar distance between the two was 3 Å and by twisting one of the PBI monomers with respect to the other by 20° along the helical axis. Visualization of the optimized geometries at the M06 and PM7 levels indicates that the PBI molecules lost their planarity within the dimer structure. Though identical in terms of energy, both P- and M-forms of the helical dimers were optimized for further model building. The interaction energy between the two monomers was calculated to be -22.45 and -36.86 kcal/mol at the M06 and PM7 levels of theory respectively indicating strong nonbonded interactions.

Similar to PBI dimer, models for the dimers of **APA** were built and were optimized at the PM7 level. Possible conformational isomers of **APA** based on the orientation of C-C single bond of alkyl chain and C-N (Adenine) have been considered to model the helices. However, only a few of these conformers can interact with the DNA strands via base pair interactions (Fig. S13). These dimers and respective monomers were subjected to geometry optimization at PM7 level and respective interaction energies were computed by taking the difference of energies between dimer and respective monomers (Table ST1). As indicated by the interaction energies, the **APA** monomers in all the four conformations can potentially aggregate to form supramolecular structures via strong non-bonded interactions. Since the P- and M-helical structures are equally preferred and are expected to be present in equal amounts, the supramolecular structures formed by only **APA** is not expected to exhibit CD signal (see Fig.2). The model systems corresponding to the **APA** and dB (B = A, T, G) hybrid assemblies were modeled using VMD. The left and

right handed DNA strands were constructed using the nucleic acid builder developed by Case and coworkers.[9] These model systems were subjected to geometry optimization by employing molecular mechanics CHARMM36 all-atom force field.[10] The geometry optimizations at the quantum mechanical level were done on the dimer steps corresponding to all the model systems using semi empirical method PM7 in MOPAC2012. The respective heat of formation values were used to calculate the Boltzmann weighted relative energies (M-P helices), which are presented in the manuscript. The Boltzmann weighted average of relative energies of the heat of formation corresponding to all the model systems considered for a particular base pair combination are provided in Fig.4 which indicate that the most stable helix for AT and AG is M-type whereas the most stable helix for AA is P-type. This is consistent with the experimental findings. Further, the absolute heat of formation values suggest that the most stable DNA assemblies formed by AT and AG are arranged in antiparallel manner whereas parallel in case of AA (Table ST2).

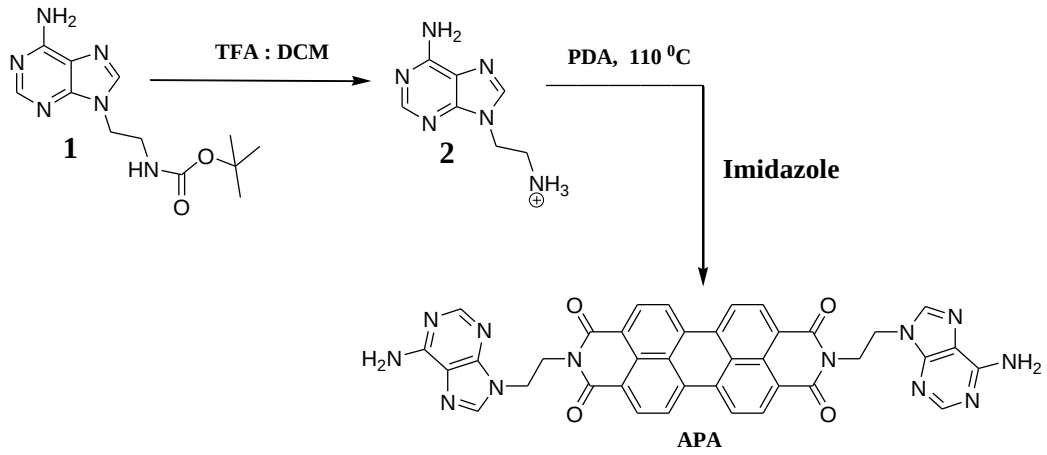

Scheme 1 Synthesis of adenine conjugated perylene bisimide (**APA**)

Preparation of APA:

Adenine derivatives **1** and **2** were prepared following the synthetic procedure from our early reports.[11] Boc-deprotected adeninyl-9-ethylamine **2** (2.2 equiv.) was added to stirred a mixture of perylene-3,4,9,10-tetracarboxylic dianhydride (PDA) (141 mg, 3.59 mmol) and imidazole (5g) at 110 ^{o}C. The reaction mixture was allowed to stir for 3 h. After completion of the reaction, the reaction mixture was cooled to room temperature. A mixture of ethanol (50 mL) and aq. HCl (1N, 50 mL) were added to the above reaction mixture and allowed to stir for 20 min. The reaction mixture was filtered and precipitate was washed with distilled water to achieve neutral pH. The obtained product (**APA**) was dried on under vacuum at 50 ºC. Brown color solid, yield 71.69 %. ^{1}H-NMR (400 MHz, *DMSO-d_6+TFA*) δ 4.53 (4H, t, J = 5.2 Hz), 4.65 (4H, t, J = 5.2 Hz), 8.21 (2H, s), 8.34 (4H, d, J = 8Hz), 8.54 (2H, s), 8.73 (4H, d, J = 8Hz), 8.93 (2H, br), 9.53 (2H, br). ^{13}C-NMR (100 MHz, *DMSO-d_6+TFA*) δ 41.2, 42.4, 118.0, 121.2, 123.6, 124.1, 127.4, 130.0, 133.0, 144.1, 144.5, 148.9, 149.9, 162.3. HRMS (ESI) found: m/z = 713.2065 $[M+H]^{+}$ and cald: 713.2122 for $C_{38}H_{25}N_{12}O_4$.

dA_{10}: 5′-AAAAAAAAAA-3′

dT_{10}: 5′-TTTTTTTTTT-3′

dG_{10}: 5′-GGGGGGGGGG-3′

dC_{10}: 5′-CCCCCCCCCC-3′

dA_{20}: 5′-AAAAAAAAAAAAAAAAAAAA-3′

dT_{20}: 5′-TTTTTTTTTTTTTTTTTTTT-3′

dG_{20}: 5′-GGGGGGGGGGGGGGGGGGGG-3′

dC_{20}: 5′-CCCCCCCCCCCCCCCCCCCC-3′

Fig. S1 Sequence information of deoxyoligonucleotides (dB_n, B = A/T/G/C) used in this study.

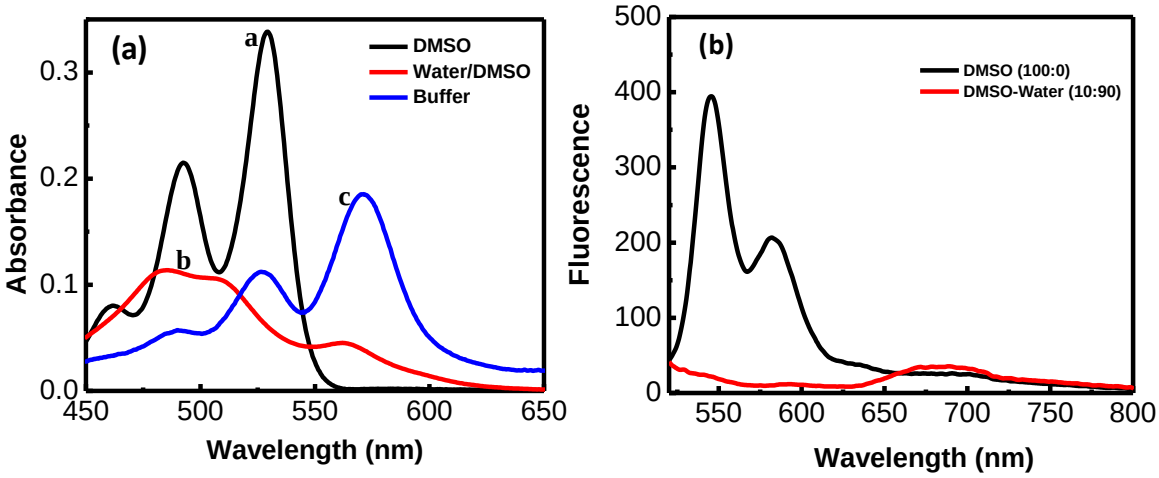

Fig. S2 UV-vis absorption and emission spectra of **APA**. **a**) **APA** in a: DMSO; b: Water/DMSO (90/10) and c: buffer/DMSO (90/10) solutions. **b**) Fluorescence spectra of **APA** (50 µM) in DMSO and aq. DMSO solution.

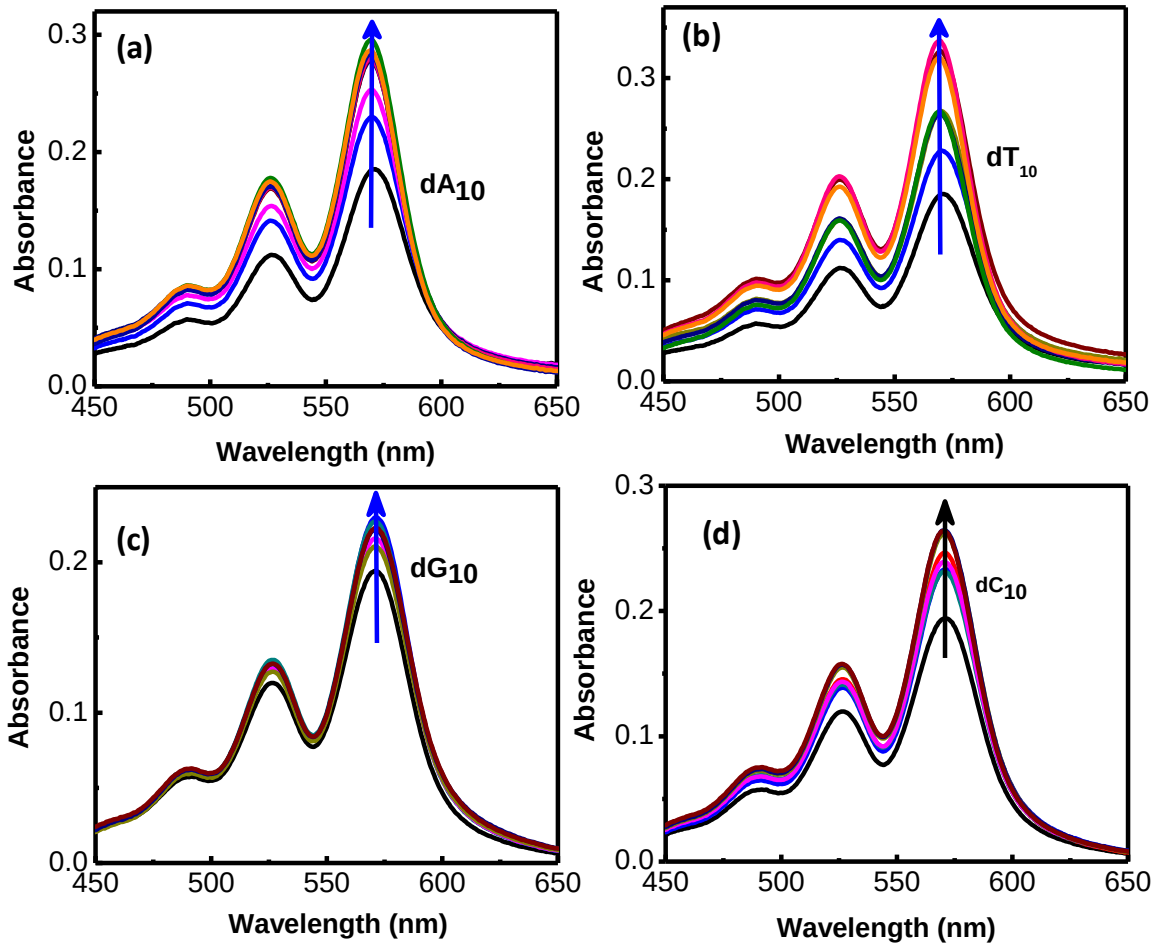

Fig. S3 UV-vis absorption spectra of **APA** with deoxyoligonucleotides (dB_n). **a**) **APA** with increasing concentration of dA_{10} in buffer solution, **b**) **APA** with increasing concentration of dT_{10} in buffer solution, **c**) **APA** with increasing concentration of dG_{10} in buffer solution and **d**) **APA** with increasing concentration of dC_{10} in buffer solution. Buffer: 10 mM, PBS containing 10% DMSO, pH = 7.

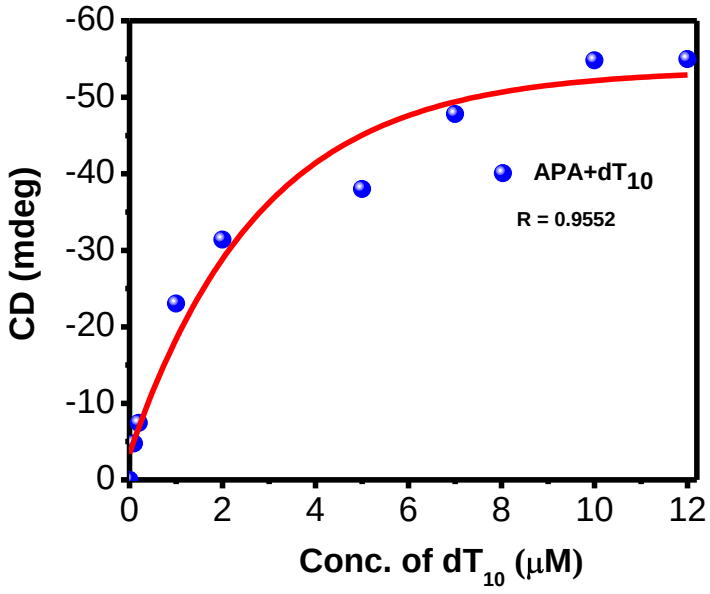

Fig. S4 CD spectra of **APA** (50 μM) with increasing concentration of dT_{10} in buffer solution.

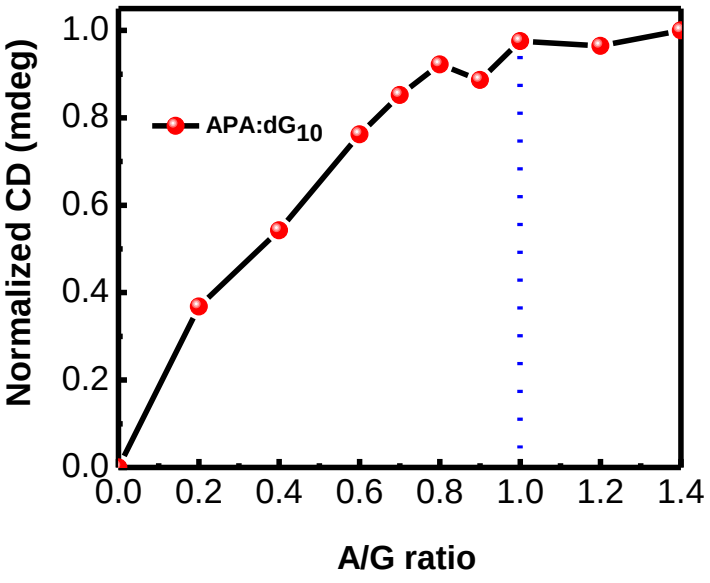

Fig. S5 Plot of CD intensity monitored at 561 nm for **APA** and dG_{10} at different combinations of **APA** against the A/G ratio at fixed concentration of dG_{10} (10 μM).

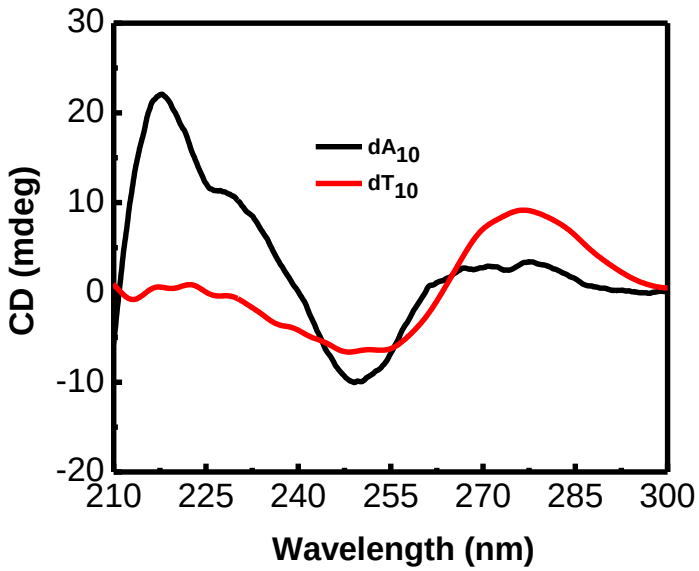

Fig. S6 CD spectra of dA_{10} and dT_{10} (10 μM) in PBS buffer solution.

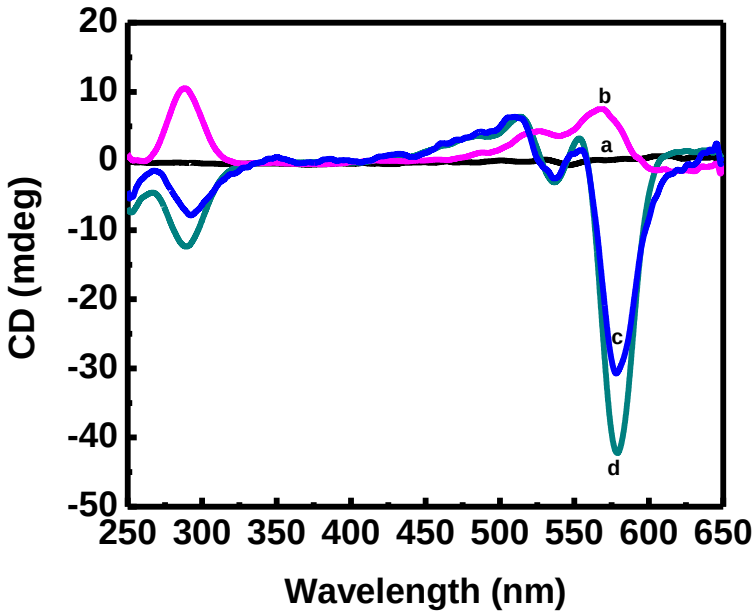

Fig. S7 CD spectra. a: **APA**, b: **APA** and dA_{20} (20:2 ratio), c: **APA** and dG_{20} (20:2 ratio), and d: **APA** and dT_{20} (20:2 ratio) in PBS buffer containing 10% DMSO, pH = 7.

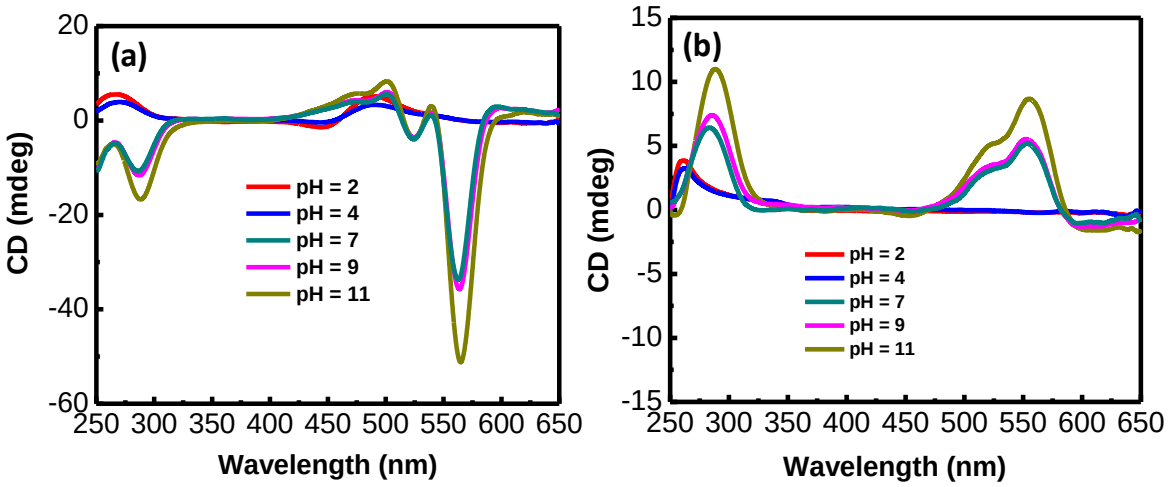

Fig. S8 pH dependent CD spectra. **a**) **APA**:dT_{20} (20:2) and **b**) **APA**:dA_{20} (20:2) in the range of pH = 2-11.

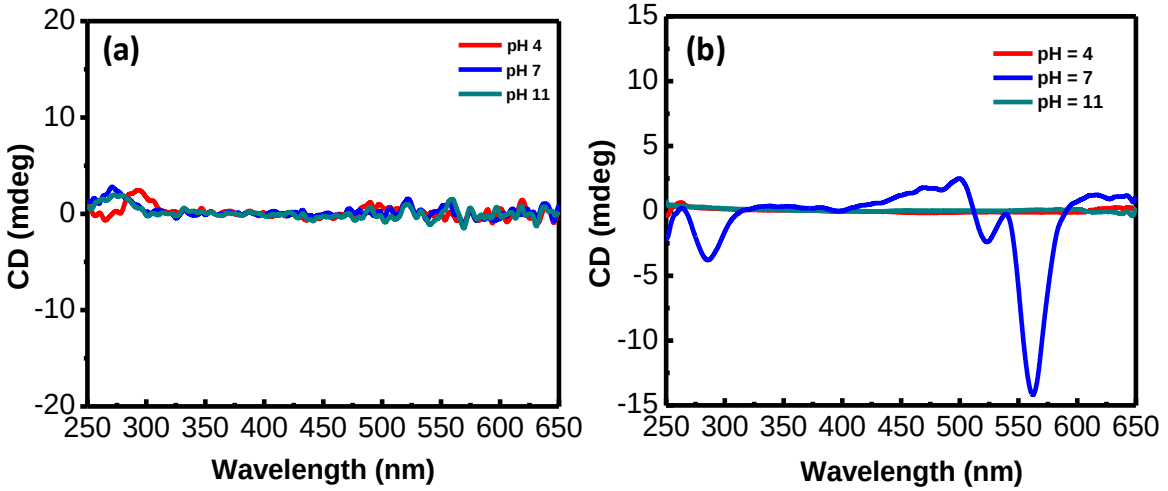

Fig. S9 pH dependent CD spectra. a) **APA**:dC_{10} (10:2) and b) **APA**:dG_{10} (10:2) in the range of pH = 4-11.

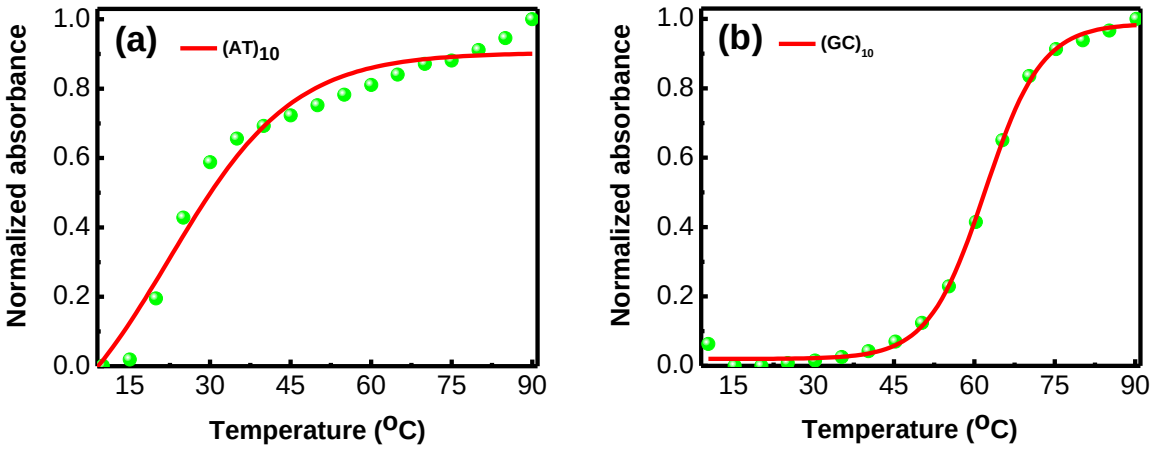

Fig. S10 Temperature dependent UV-vis spectra of dsDNA monitored at 260 nm. **a**) & **b**) are melting curves of $(AT)_{10}$ and $(GC)_{10}$ duplexes in the absence of **APA**.

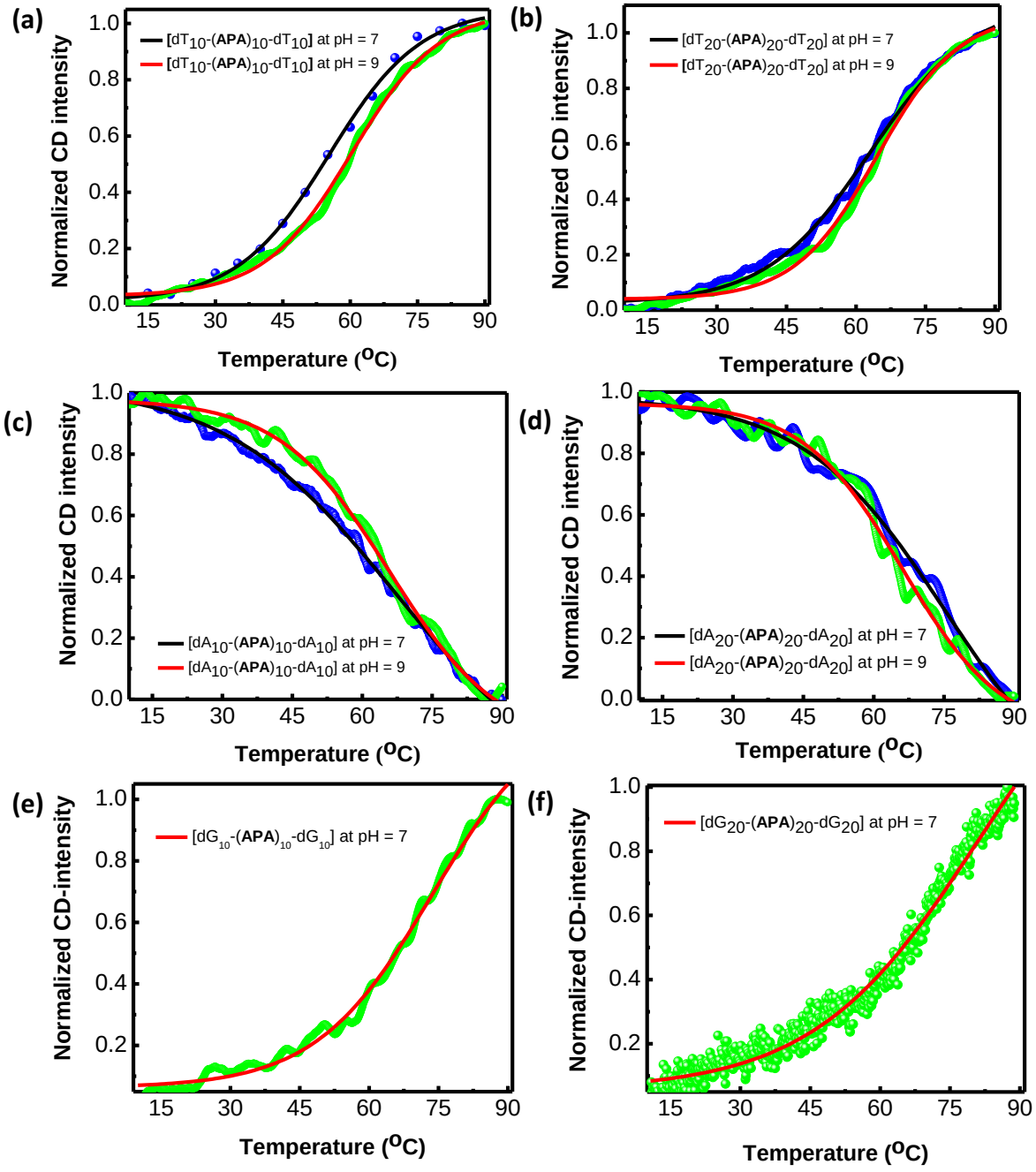

Fig. S11 Temperature dependent CD spectra of [dB_n:(**APA**)$_n$:dB_n] ensembles monitored at 561 nm corresponds to perylene absorption. **a**) & **b**) Melting curves for the binary complexes of dT_{10} and dT_{20} with **APA** at pH = 7 and 9 respectively. **c**) & **d**) Melting curves for the binary complexes of dA_{10} and dA_{20} with **APA** at pH = 7 and 9 respectively. **e**) & **f**) Melting curves for the binary complexes of dG_{10} and dG_{20} with **APA** at pH = 7 respectively.

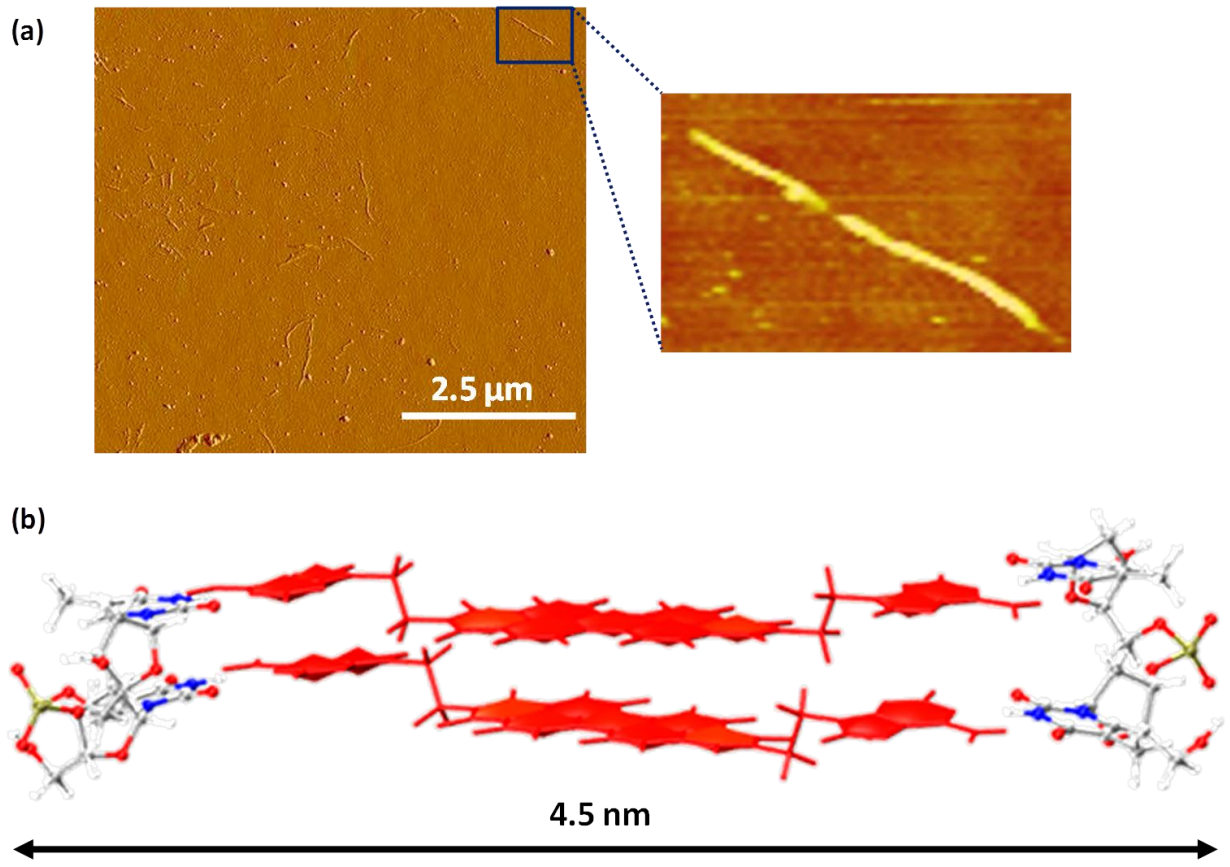

Fig. S12 a) AFM image of left-handed helical DNA ensembles of [dT_{20}-(**APA**)$_{20}$-dT_{20}]. High resolution image (rectangle) shows the isolated left-handed helical assembly structures of [dT_{20}-(**APA**)$_{20}$-dT_{20}]. **b**) Typical thickness (4.5 nm) of [dT_{20}-(**APA**)$_2$-dT_{20}] calculated from theoretical model.

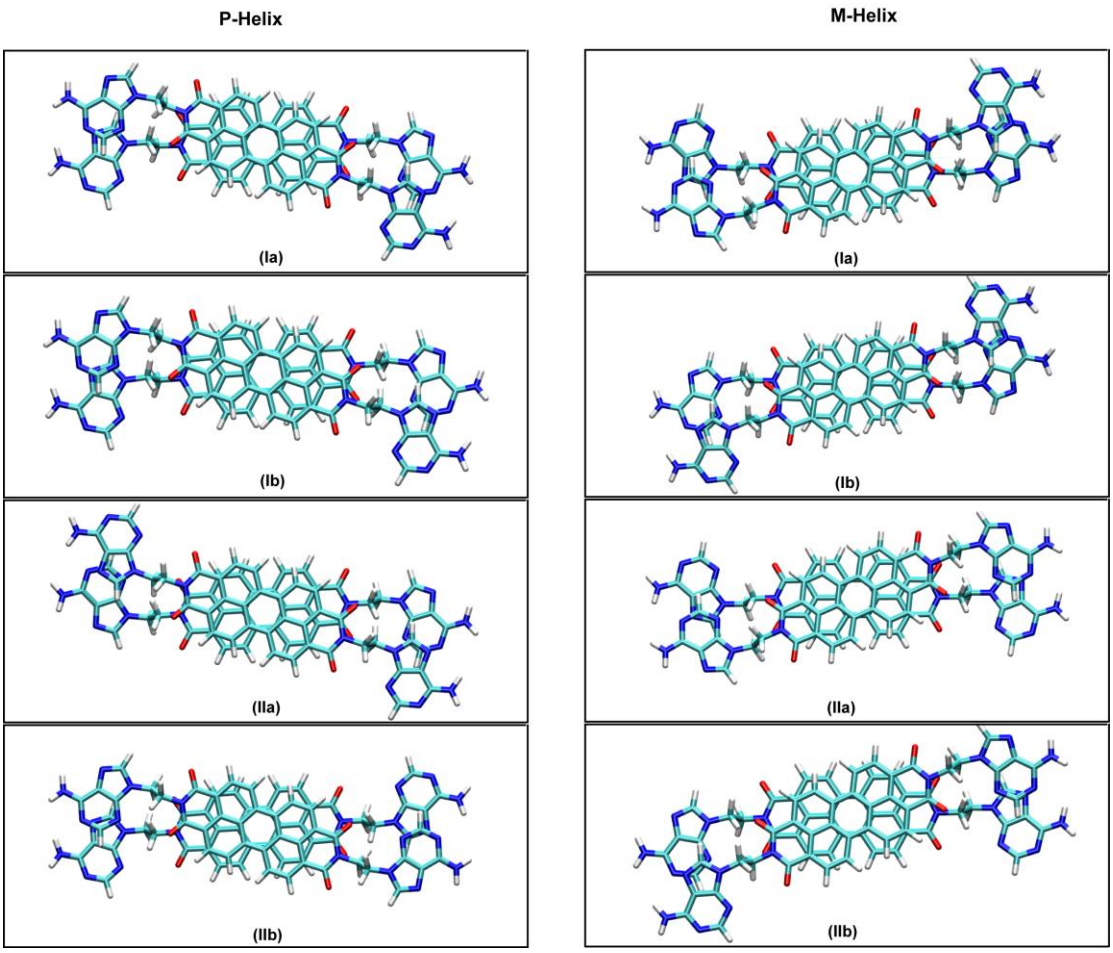

Fig. S13 Various possible conformers for **APA** dimers in M- and P-helices which form antiparallel (Ia, Ib) and parallel (IIa, IIb) helices when interacted with deoxyoligonucleotides dB_n (B=A, T, G).

Table. ST1 Interaction energies (in kcal/mol) of PBI and **APA** dimers in various conformations calculated by using PM7 method in MOPAC2012. Interaction energy corresponding to PBI dimer at M06 level is also specified.

Structure	Interaction energy
PBI dimer	-36.86 (-22.45)
A-PBI-A dimer	
Ia	-62.25
Ib	-64.05
IIa	-59.59
IIb	-65.11

Table ST2: Heat of formation values of M- and P- helices at dimeric steps level in several orientations comparing two antiparallel (Ia, Ib) and the two parallel (IIa, IIb) for both M- and P-type helices (see **Fig. S13**).

Helix type	Orientation	A:T (WW)	A:A (WW)	A:G (WW)
M-Helix	Ia	-1280.3	-645.0	-874.6
	Ib	-1270.1	-681.9	-895.9
	IIa	-1275.2	-675.0	-833.0
	IIb	-1279.5	-683.5	-851.3
P-Helix	Ia	-1268.1	-673.1	-842.2
	Ib	-1249.3	-688.8	-846.0
	IIa	-1274.5	-694.7	-846.1
	IIb	-1257.1	-634.2	-806.4

Fig. S14 Final structures corresponding to the most stable P- and M-duplexes obtained after geometry optimization using semi empirical PM7 method. The hydrogen bond distances (in Å) were given below of each of the geometry. The first and second lines represent hydrogen bonds in 5'-3' and 3'-5' strands respectively.

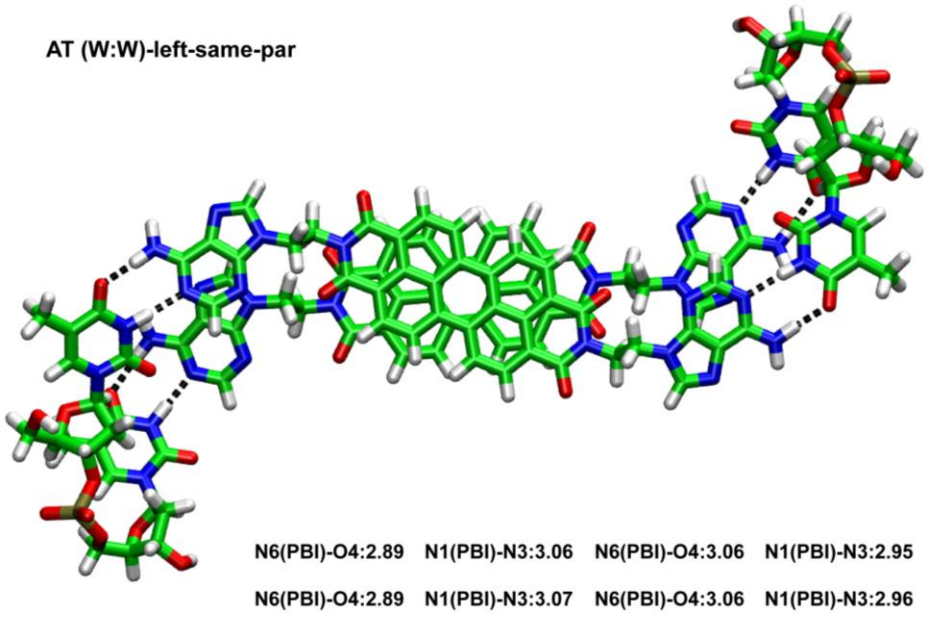

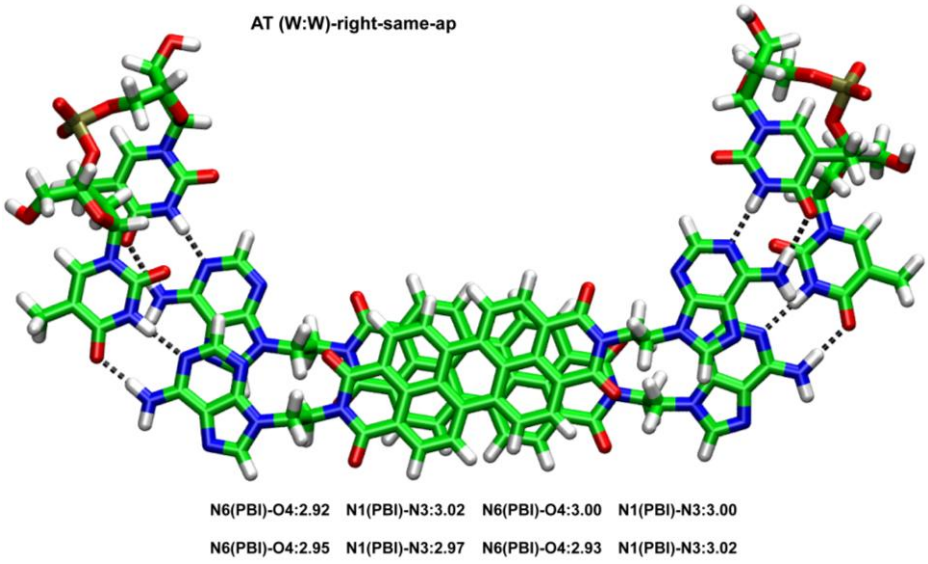

AA (W:W)-left-oppos-par

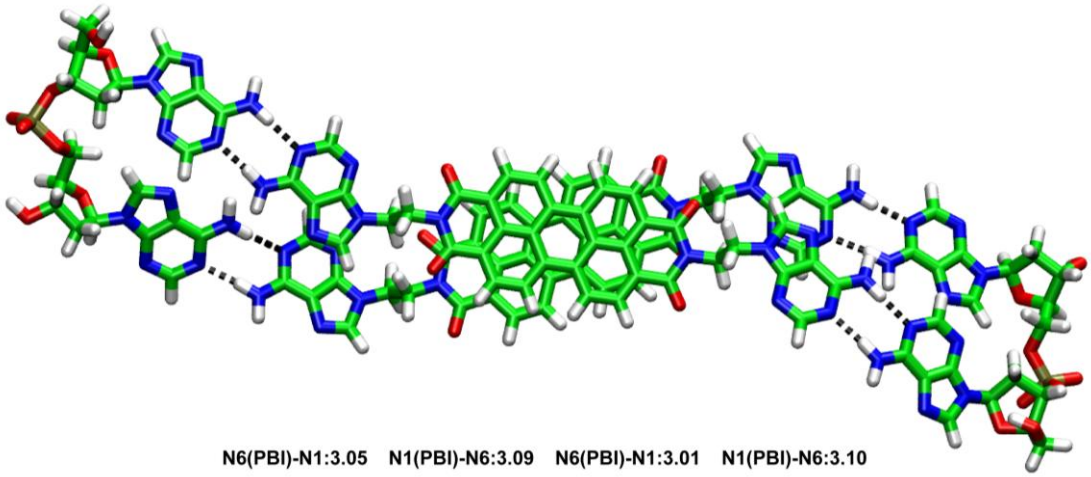

N6(PBI)-N1:3.05 N1(PBI)-N6:3.09 N6(PBI)-N1:3.01 N1(PBI)-N6:3.10
N6(PBI)-N1:2.99 N1(PBI)-N6:3.16 N6(PBI)-N1:3.08 N1(PBI)-N6:3.08

AA (W:W)-right-same-ap

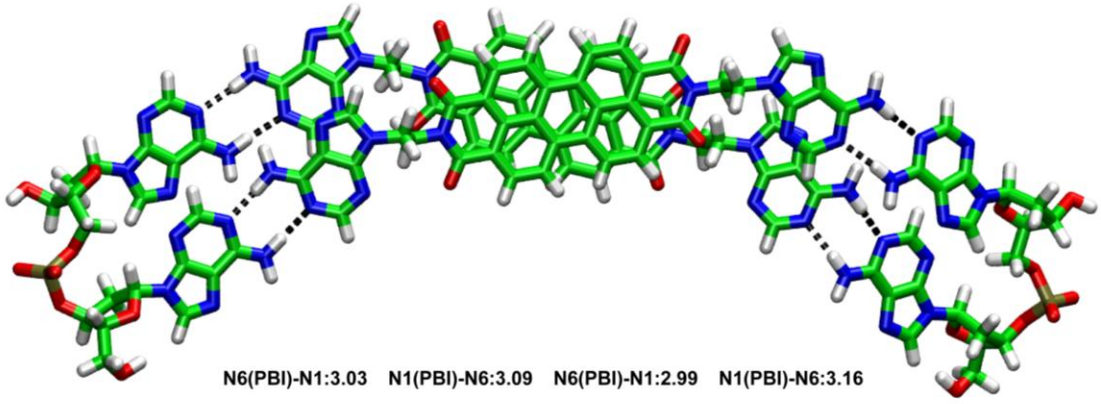

N6(PBI)-N1:3.03 N1(PBI)-N6:3.09 N6(PBI)-N1:2.99 N1(PBI)-N6:3.16
N6(PBI)-N1:3.02 N1(PBI)-N6:3.10 N6(PBI)-N1:3.00 N1(PBI)-N6:3.16

AG (W:W)-left-oppos-ap

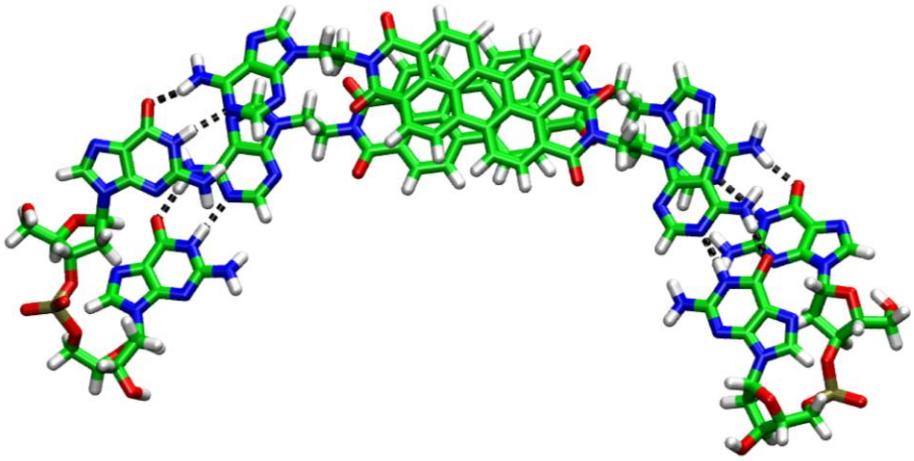

N6(PBI)-O6:2.89 N1(PBI)-N1:2.99 N6(PBI)-O6:2.92 N1(PBI)-N1:3.08

N6(PBI)-O6:2.82 N1(PBI)-N1:3.07 N6(PBI)-O6:2.99 N1(PBI)-N1:3.08

AG (W:W)-right-same-par

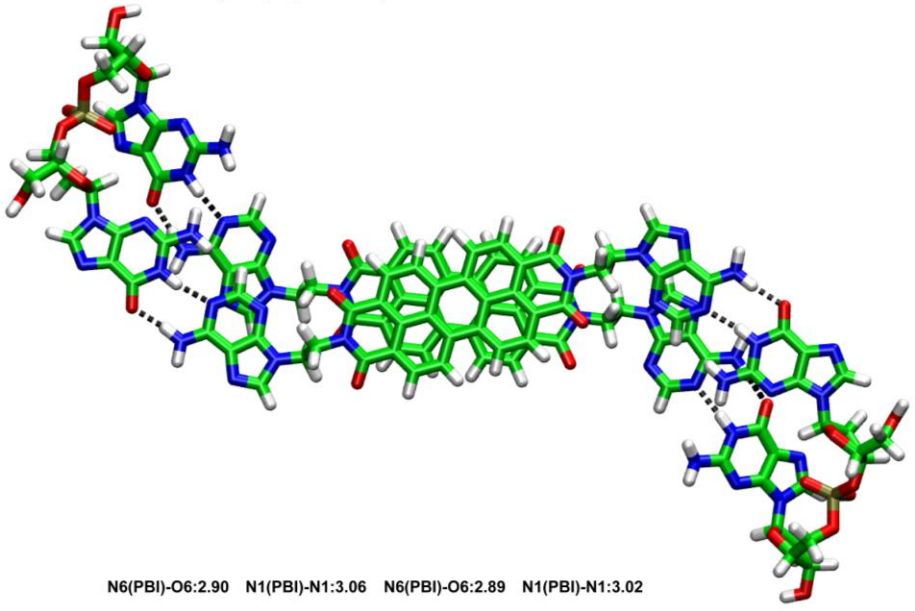

N6(PBI)-O6:2.90 N1(PBI)-N1:3.06 N6(PBI)-O6:2.89 N1(PBI)-N1:3.02

N6(PBI)-O6:2.90 N1(PBI)-N1:3.05 N6(PBI)-O6:2.88 N1(PBI)-N1:3.02

References

1. (a) K. Rippe, *Futura* 1997, **12**, 20−26; (b) P. G. A. Janssen, S. Jabbari-Farouji, M. Surin, X. Vila, J. C. Gielen, J. T. F. A. de Greef, M. R. J. Vos, P. H. H Bomans, N. A. J. M. Sommerdijk, P. C. M. Christianen, Leclère, Ph., R. Lazzaroni, P. van der Schoot, E. W. Meijer and A. P. H. J. Schenning, *J. Am. Chem. Soc.* 2009, **131**, 1222– 1231.
2. R. Dennington, T. Keith and J. Millam, *Semichem Inc.*, Shawnee Mission KS, *GaussView Version 5*, 2009.
3. W. Humphrey, A. Dalke and K. Schulten, *J. Molec. Graphics*., 1996, **14**, 33-38.
4. Y. Zhao and D. G. Truhlar, *Theor. Chem. Acc*., 2008, **120**, 215-241.
5. M. J. Frisch, G. W. Trucks, H. B. Schlegel, G. E. Scuseria, M. A. Robb, J. R. Cheeseman, G. Scalmani, V. Barone, B. Mennucci, G. A. Petersson, H. Nakatsuji, M. Caricato, X. Li, H. P. Hratchian, A. F. Izmaylov, J. Bloino, G. Zheng, J. L. Sonnenberg, M. Hada, M. Ehara, K. Toyota, R. Fukuda, J. Hasegawa, M. Ishida, T. Nakajima, Y. Honda, O. Kitao, H. Nakai, T. Vreven, J. A. Montgomery, Jr., J. E. Peralta, F. Ogliaro, M. Bearpark, J. J. Heyd, E. Brothers, K. N. Kudin, V. N. Staroverov, R. Kobayashi, J. Normand, K. Raghavachari, A. Rendell, J. C. Burant, S. S. Iyengar, J. Tomasi, M. Cossi, N. Rega, J. M. Millam, M. Klene, J. E. Knox, J. B. Cross, V. Bakken, C. Adamo, J. Jaramillo, R. Gomperts, R. E. Stratmann, O. Yazyev, A. J. Austin, R. Cammi, C. Pomelli, J.W. Ochterski, R. L. Martin, K. Morokuma, V. G. Zakrzewski, G. A. Voth, P. Salvador, J. J. Dannenberg, S. Dapprich, A. D. Daniels, Ö. Farkas, J. B. Foresman, J. V. Ortiz, J. Cioslowski and D. J. Fox, Gaussian 09, Revision C.01, Gaussian, Inc., Wallingford CT, 2009.
6. J. J. Stewart, *J. Mol. Model.*, 2013, **19**, 1-32.
7. J. J. P. Stewart, Stewart Computational Chemistry, Colorado Springs, CO, USA, MOPAC2012, 2012, 151.
8. (a) Y. Zhao and D. G. Truhlar, *Phys Chem Chem Phys.*, 2008, **10**, 2813-2818; (b) S. Manchineella, V. Prathyusha, U. D. Priyakumar and T. Govindaraju, *Chem. Eur. J.*, 2013, **19**, 16615-16624.

9. T. Macke and D. A. Case, *Modeling unusual nucleic acid structures. In Molecular Modeling of Nucleic Acids*, N.B. Leontes and J. SantaLucia, Jr., eds. (Washington, DC: American Chemical Society), **1998**, 379-393.
10. (a) B. R. Brooks, C. L. III. Brooks, A. D. Jr. Mackerell, L. Nilsson, R. J. Petrella, B. Roux, Y. Won, G. Archontis, C. Bartels, S. Boresch, A. Caflisch, L. Caves, Q. Cui, A. R. Dinner, M. Feig, S. Fischer, J. Gao, M. Hodoscek, W. Im, K. Kuczera, T. Lazaridis, T. Ma, V. Ovchinnikov, E. Paci, R. W. Pastor, C. B. Post, J. Z. Pu, M. Schaefer, B. Tidor, R. M. Venable, H. L. Woodcock, X. Wu, W. Yang, D. M. York and M. Karplus, *J. Comput. Chem.*, 2009, **30**, 1545–1614; (b) A. D. Jr. MacKerell and N. K. Banavali, *J. Comput. Chem.*, 2000, **21**, 105–120; (c) E. J. Denning, U. D. Priyakumar, L. Nilsson and A. D. Jr. MacKerell, *J. Comp. Chem.*, 2011, **32**, 1929-1943.
11. N. Narayanaswamy, M. B. Avinash and T. Govindaraju, *New J. Chem.*, 2013, **37**, 1302-1306.

^{1}H-NMR spectra of APA

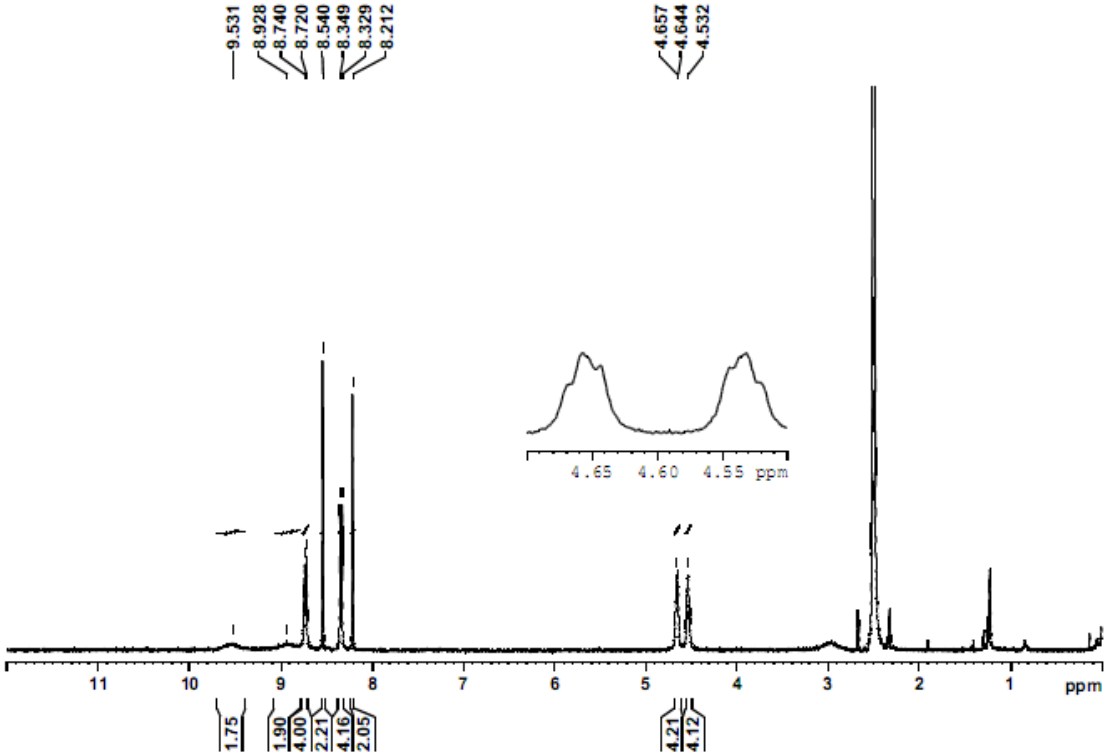

^{13}C-NMR spectra of APA